Hemophagocytic lymphohistiocytosis as an onset of diffuse large B-cell lymphoma: A case report

YUEQING CAO[1-3], LANG ZOU[1-3], HAO ZHOU[1-3], GAN FU[1-3] and XIELAN ZHAO[1-3]

[1]Department of Hematology, Xiangya Hospital, Central South University;
[2]National Clinical Research Center for Geriatric Diseases (Xiangya Hospital);
[3]Hunan Hematology Oncology Clinical Medical Research Center, Changsha, Hunan 410008, P.R. China

Received January 4, 2022; Accepted May 19, 2022

DOI: 10.3892/ol.2022.13418

Abstract. A 53-year-old male presented with a 1-month history of hyperpyrexia. The clinical manifestations revealed hemophagocytic lymphohistiocytosis (HLH). Although a lymph node biopsy could not be obtained, a bone marrow biopsy revealed the activated B-cell subtype of diffuse large B-cell lymphoma (DLBCL). After being treated with HLH-1994 (dexamethasone and etoposide), a rituximab-containing chemotherapy and target agents involving bortezomib, the patient achieved remission. To understand the molecular profile of patient, next-generation sequencing and MYD88 L265P mutation examinations were performed, and the patient was determined to be positive for the MYD88 L265P mutation. Reports of DLBCL with plasmacytic differentiation and a MYD88 innate immune signal transduction adaptor L265P mutation concurrent with HLH are rare. Early recognition, precise diagnosis and timely therapy are pivotal in improving patient prognosis. Furthermore, molecular profiling enables researchers to develop potential therapies aimed at the activated NF-κB and endoplasmic reticulum stress signaling pathways. The present study highlights this pathogenesis and provides suggestions for further individualized therapeutics.

Introduction

Hemophagocytic lymphohistiocytosis (HLH) is a fatal and hyperinflammatory disorder associated with excessive activation of cytotoxic T cells, natural killer (NK) cells and macrophages. Failure to control the immune response leads to marked elevation of cytokines, inducing systemic inflammatory symptoms and signs (1). While primary HLH is caused by genetic defects in proteins affecting the release of cytolytic granules, perforin1, unc-13 homolog D, syntaxin binding protein 2, syntaxin 11, SH2 domain containing 1A, Rab27a or X-linked inhibitor of apoptosis gene mutations are commonly detected among patients with primary HLH (2). Secondary HLH can occur due to environmental triggers, including severe infectious and non-infectious factors (autoimmunity, malignancy, drugs, pregnancy and others) (2,3). Patients with HLH frequently present with inflammatory infiltration manifestations characterized by fever, cytopenia, coagulopathy, organomegaly (splenomegaly, hepatomegaly, lymphadenopathy), liver dysfunction (elevated transaminases and bilirubin), hemophagocytosis, hypertriglyceridemia, hyperferritinemia, increased serum soluble interleukin-2 receptor/CD25 and diminished NK cell function. The most widely accepted diagnostic criteria for HLH are the HLH-2004 criteria (4), which are based on the aforementioned clinical manifestations. As the purpose of therapy is to limit the uncontrolled immune response, the mainstay of therapy includes immunosuppressive and myelosuppressive drugs, most frequently dexamethasone and etoposide, according to two landmark studies performed in the pediatric HLH population (4). It is considered that timely recognition of the underlying disease and accurate treatment to control the trigger are necessary to decrease mortality rates (3).

Diffuse large B-cell lymphoma (DLBCL) accounts for 30-35% of newly diagnosed B-cell lymphomas (5). Although DLBCL is curable with first-line treatment of rituximab plus cyclophosphamide, doxorubicin, vincristine and prednisone (R-CHOP) in >60% of patients, the remaining patients develop relapsed/refractory (RR) disease. However, in transplant ineligible patients with RR, management is almost palliative, and salvage regimens are limited due to toxicities (6). Chimeric antigen receptor T-cell therapy with anti-CD19 products has obtained encouraging results, but notable toxicities and economic challenges have restricted its usage. With the advent of genome-wide molecular profiling, targeted strategies such as ibrutinib, bortezomib (BTZ), and lenalidomide are promising, and numerous trials exploring combinations of agents are underway (7-10). Notably, a growing body of evidence suggests that innovative approaches linking individual molecular profiles to the

Correspondence to: Dr Gan Fu or Dr Xielan Zhao, Department of Hematology, Xiangya Hospital, Central South University, 87 Xiangya Road, Changsha, Hunan 410008, P.R. China
E-mail: gannffu@tom.com
E-mail: zhaoxl9198@163.com

Key words: hemophagocytic lymphohistiocytosis, diffuse large B-cell lymphoma, bortezomib, bone marrow biopsy, NF-κB signaling pathway, myeloid differentiation primary response 88 L265P

efficacy of single agents or an 'R-CHOP plus' (R-CHOP with additional drugs) regimen underscore awareness about how to select patients who will benefit from this type of extension of the standard therapy (11).

As B-cell lymphoma with HLH is seldom reported, to the best of our knowledge, this is the first report of a case of HLH as a prelude to activated B-cell-like DLBCL (ABC DLBCL), which was accompanied by plasmacytic differentiation and a MYD88 innate immune signal transduction adaptor L265P (MYD88 L265P) mutation. It was assumed that the mutation of MYD88 L265P and plasmacytic differentiation resulted in activation of the endoplasmic reticulum (ER) stress and NF-κB signaling pathways. Understanding the pathogenesis enables researchers to develop novel intervention strategies for patients with activated NF-κB and ER stress signaling pathways, proposing a safe and feasible way to enhance outcomes in this subset of patients.

Case report

Case. A 53-year-old male was admitted to Xiangya Hospital (Central South University, Changsha, China) with a 1-month history of hyperpyrexia in June 2018. Upon admission, the vital signs included a temperature of 37.5˚C, a heart rate of 96 beats/min, a blood pressure of 110/50 mmHg, and a respiratory rate of 20 breaths/min. Physical examination revealed an anemic appearance but no palpable lymphadenopathy. An initial workup showed acute inflammatory deterioration [C reactive protein, 69.3 mg/l (normal, 0-8 mg/dl); procalcitonin, 0.88 ng/ml (normal, 0-0.1 ng/ml); anemia [hemoglobin level, 5.4 g/dl (normal, 13-17.5 g/dl)], thrombocytopenia [platelet level, $25x10^3/\mu l$ (normal, $100-300x10^3/\mu l$)], hypertriglyceridemia [triglyceride level, 3.47 mmol/l (normal, 0-1.7 mmol/l)] and increased ferritin [>2,530 μg/l (normal, 16-400 μg/l)]. Moreover, the patient had elevated immunoglobulin levels [IgM, 5,010 mg/l (normal, 400-2,800 mg/l)]. Simultaneously, both serum and urine electrophoresis detected IgM κ chains. B-mode ultrasound imaging of the superficial lymph nodes showed multiple lymph nodes on both sides of the cervical region, axillary fossa and groin, but none were larger than 13x4 mm. A computed tomography (CT) scan revealed multiple mesentery lymph nodes and splenomegaly. Notably, bone marrow aspiration showed hemophagocytosis (data not shown).

According to HLH-2004, a diagnosis of secondary HLH could be made as the patient had 5 out of 8 parameters (bicytopenia, splenomegaly, hypertriglyceridemia, hyperferritinemia and hemophagocytosis) (4). According to the HLH-1994 protocol, standard care for children with HLH is a combination of etoposide and dexamethasone (12). The HLH-2004 chemotherapy protocol, which was modified from HLH-1994, added cyclosporine A during the initial therapy phase. Some previous studies have suggested that adding cyclosporine offers no clinical advantage, and the present patient started with the HLH-1994 protocol. After the first cycle of therapy, the general condition of the patient improved gradually, and no abnormal signs were observed during a physical examination, except anemia. The values of the blood cells were elevated markedly (hemoglobin level, 6.9 g/dl; platelet level, $10.2x10^4/\mu l$). Therefore, the patient only underwent one cycle of HLH-1994. Further investigations and positron emission tomography (PET)/CT revealed multiple bone parenchyma, spleen and both adrenal glands with increased glucose metabolism, which was mostly due to lymphoma infiltration (Fig. 1A). According to the PET/CT results, bilateral bone marrow biopsies were collected. While the pathological results of the right posterior superior iliac spinal biopsy revealed proliferative changes, the left side showed diffuse large B-cell lymphoma that conformed to the ABC type described by Hans *et al* (13) upon immunohistochemical analysis, which showed the following results: $CD20^+$, paired box 5^+, $Bcl\text{-}6^+$, multiple myeloma 1^+, $Bcl\text{-}2^+$ (50%), $C\text{-}myc^+$ (10%) and $Ki67^+$ (50%) (Fig. 2). Flow cytometry showed that there were 3.1% mature clonal B cells among karyocytes, and these cells were positive for CD45, CD19, CD20 and sκ, and negative for CD38, CD10 and sλ (Fig. 3). The chromosome karyotype analysis result was 46, XY. As IgM κ M proteins were detected both in serum and urine electrophoresis, fluorescence *in situ* hybridization (FISH) analysis was performed for multiple myeloma (MM) chromosomal translocations of t(14;16)(q32;q23), t(4;14)(q16;q32) and t(11;14)(q13;q32), which are likely to cause gene overexpression of MAF BZIP transcription factor (MAF), FGFR3 and cyclin D1 (CCND1), respectively (14). All the aforementioned translocations were negative (Fig. 4). Further FISH analysis results demonstrated negative results for the 1q21/RB transcriptional corepressor 1 (RB1), D13S319/TP53, immunoglobulin heavy locus (IGH), T-cell receptor α/δ (TCRAD) and T-cell receptor β (TCRB) genes (Fig. 4). However, Ig VH, Ig DH, Ig K and Ig L gene rearrangements were detected (data not shown). None of the explicit mutations associated with hematological malignancies were revealed by next-generation sequencing (NGS), but allele-specific PCR discovered that the patient was positive for the MYD88 L265P gene mutation. The inconformity of these two tests may be due to the limitations of NGS, including analytic sensitivity of mutation detection or areas of the genome that are difficult to sequence (15). Consequently, the diagnosis of the patient was DLBCL [ABC type, stage IVB; International Prognostic Index (IPI) score, 4; CNS score, 5; plasmacytoid differentiation; and MYD88 L265P mutation]. The patient therefore did not undergo an HLH genetic study due to the increased likelihood that HLH was secondary to DLBCL.

Although R-CHOP is the frontline standard of care for DLBCL, among patients with RR DLBCL, less favorable outcomes have prompted efforts to improve first-line approaches. EPOCH-R, a 96-h continuous infusion regimen of R-CHOP that incorporates a dynamic dose adjustment, has shown excellent efficacy in Bcl-2-positive DLBCL (16). With the consideration that the present study patient was Bcl-2-positive with multiple organ infiltration, EPOCH-R was chosen for the patient to prevent recurrence. As the lymphoma was likely to be accompanied by plasmacytic differentiation, the patient received intensive regimens of high-dose methotrexate (to prevent intracranial involvement, as the abnormal adrenal gland was presumed to be lymphoma infiltration) based on the combination chemotherapy of rituximab and BTZ. The detailed timeline of treatments is shown in Fig. 5.

Since the collection of stem cells from the bone marrow failed, ibrutinib or lenalidomide administration was recommended. The patient selected lenalidomide (25 mg daily) for maintenance treatment. The last PET/CT performed in February 2019 showed that glucose metabolism, which was

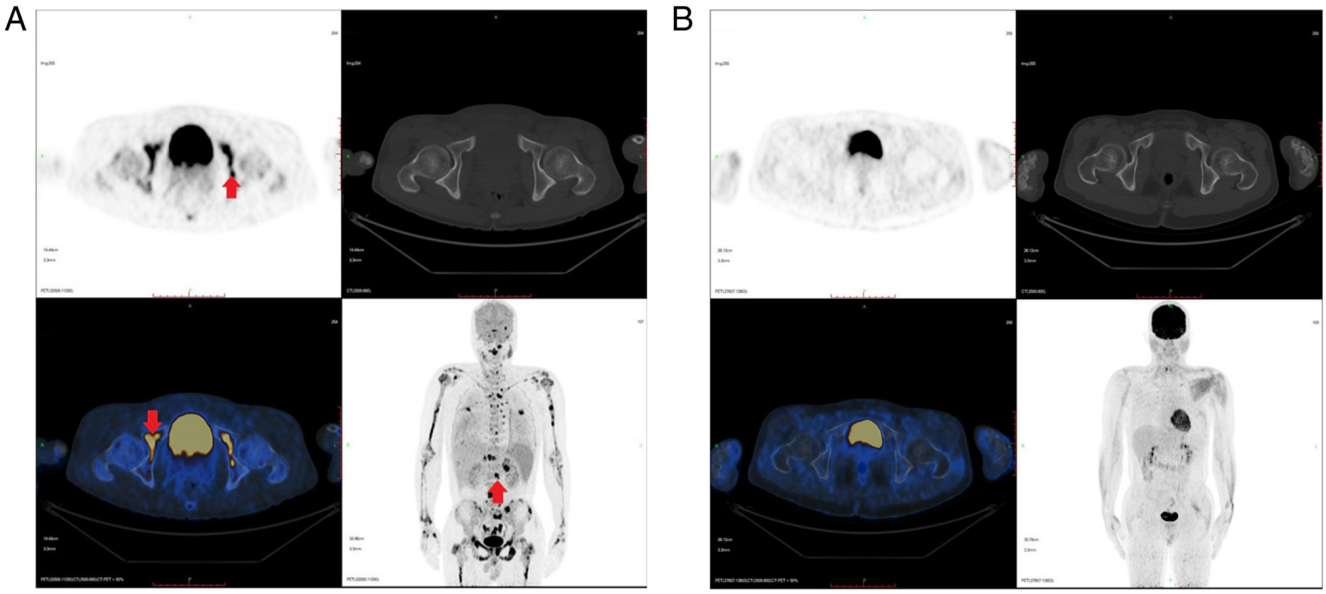

Figure 1. PET-CT at diagnosis of lymphoma and at completion of 4 cycles of chemotherapy. (A) Initial PET-CT revealed increased glucose metabolism of multiple bone parenchyma suggesting lymphoma infiltration (red arrows). (B) PET-CT scans performed after 4 cycles of chemotherapy were negative for residual disease. PET-CT, positron emission tomography-computed tomography.

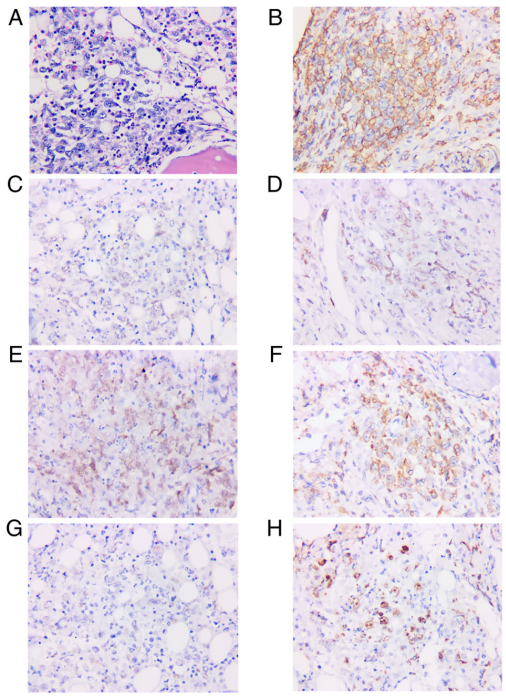

Figure 2. Pathological findings of bone marrow biopsy are diffuse large B-cell lymphoma. (A) Hematoxylin and eosin staining patterns revealing diffuse, pleomorphic, medium to large tumor cell infiltration (magnification, x400). Immunohistochemical staining patterns showing tumor cells positive for (B) CD20, (C) paired box 5, (D) Bcl-6, (E) multiple myeloma ongogene 1, (F) Bcl-2, (G) c-myc, and (H) Ki67 (magnification, x400).

originally increased in multiple bone parenchyma, the spleen and both adrenal glands, was generally ameliorated, which indicated complete remission (CR) of the lymphoma (Fig. 1B). The patient is being followed up by the Department of Hematology in Xiangya Hospital every 6 months, and currently remains free of disease with quiescent HLH.

Imaging examinations. The plain and contrast-enhanced CT scans of the chest, abdomen and pelvis were made with the Aquilion ONE 320-detector row CT scanner (Canon Medical Systems Corporation). The CT parameters were as follows: 120 kV, automatic mAsec, 1.0-mm thickness, 1.0-mm intervals and a matrix of 256x256. The PET/CT scans were performed on a GE Discovery 690 PET/CT scanner (GE Healthcare).

FISH analysis. Interphase FISH analysis was performed according to the standards of the International System for Human Cytogenetic Nomenclature 2016 (17). The bacterial artificial chromosome (BAC) DNA clones were purchased from Children's Hospital Oakland Research Institute and were separated into individual colonies on a Luria Broth (LB) agar plate (18). The colonies were inoculated in 10 ml LB with appropriate antibiotics, incubated at 37˚C and agitated at 250 rpm. The bacteria were collected by centrifugation at 3,000 x g for 10 min at 4˚C. Next, high-purity BAC DNA was extracted using the NucleoBond PC20 kit (cat. no. 740519.20; Machery-Nagel). After digesting BAC plasmids with restriction endonuclease *Bam*HI (cat. no. 81295-09-2; MilliporeSigma) at 37˚C for >2 h, DNA bands were separated by electrophoresis on a 1% agarose gel and using 1X Tris-acetate-EDTA (TAE) buffer at 20-30 V to identify each clone by further FISH. The BAC clones were stored in LB and glycerol at a ratio of 1:1 and kept at -80˚C. The BAC DNA was labeled by 50 μl reaction mixture using a Nick Translation Reaction kit (cat. no. 07J00-001; Abbot Pharmaceutical, Co., Ltd.), then incubated at 15˚C for 1-2 h and at 70˚C for 10 min. The Nick Translation products were separated with 1.5% agarose gel and 1X TAE buffer, at 70-100 V for ≥1 h. After precipitation, DNA probes were collected at 17,000 x g in a benchtop centrifuge at 4˚C for 30 min, then washed and air-dried. DNA probes were suspended in 100 μl *in situ* Hybridization Kit BioAssay (cat. no. I7643-50H; United States Biological). After denaturation at 75˚C for 10 min, blocking of non-specific genomic sequences was performed at

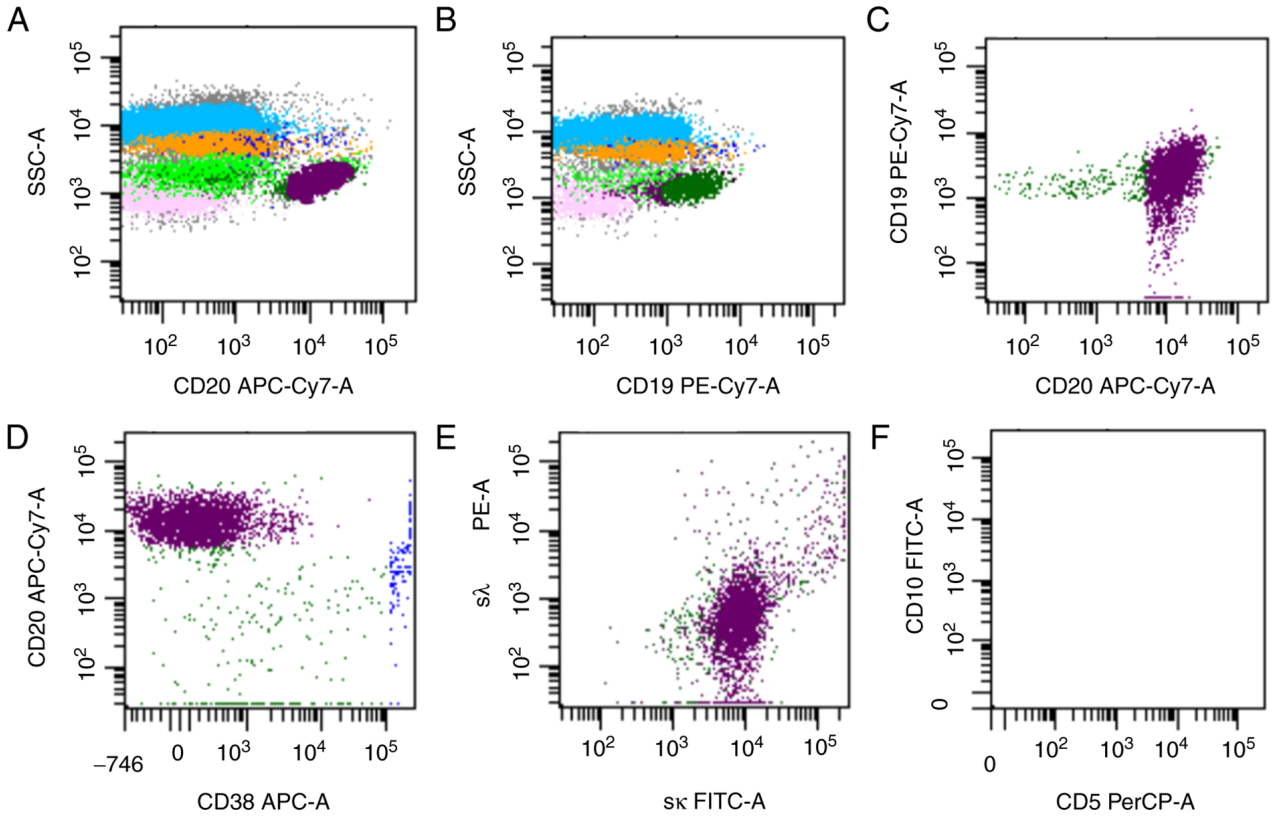

Figure 3. Flow cytometry analysis of the bone marrow. (A) The large cells were positive for CD45 (purple cell cluster of ~3.1%). (B) There were 3.1% CD19-positive cells (bottle green cell cluster). (C) 3.1% of cells were positive for CD19 and CD20 (bottle green/purple cell cluster). (D) Cells positive for CD20 (purple cell cluster of ~3.1%) and negative for CD38. (E) The cells were positive for sκ (purple cell cluster ~91%) and negative for sλ. (F) The mature B cells were negative for both CD5 and CD10. Dark grey, impurities; light green, lymphoid cells; light grey, immature cells; blue, neutrophils; orange, monocytes; pink, karyocytes; bottle green, CD19-positive cells; purple, CD45/CD20 and sκ-positive cells

37˚C for 30 min. Finally, the probes were stored at -20˚C. Bone marrow aspirate samples were mixed with EDTA immediately once collected. RPMI-1640 medium + 5% fetal bovine serum at a 1:1 or 1:5 ratio was added to bone marrow for removing erythrocytes. Diluted cells were laid onto Histopaque-1077 medium (cat. no. 397639117; MilliporeSigma). Next, cells were centrifuged at 1,800-2,000 x g for 25 min at room temperature (RT). Leukocytes were harvested, washed with RPMI-1640 medium and then counted. A glass coverslip was used and washed with PBS once, and then 0.1 ml of purified lymphocytes from the patient was added and centrifuged for 5 min at 1,000 x g at RT. Plates were put on a clean bench for 30 min at RT. Slides were fixed at 37˚C in a dry oven overnight and stored at -20˚C. For FISH, the chromosomal DNA was denatured on the slides in 90% formamide/2X SSC solution at 37˚C for 8 min. The slides were dehydrated and then air-dried. The hybridization mixture containing fluorochrome red and green probes was added to the slides, covered with a cover slip and incubated in moist plastic chambers at RT for 1 h. Slides were incubated in the Hybrite thermal plate (MilliporeSigma) at 75˚C for denaturation and hybridization. Next, slides were washed, dried and then immersed in 1X PBS for 3 min at RT. The semidried slides were treated with 100 μl of 1:20 light chain (κ or λ) antibody staining dilute AMCA goat-antibody (cat. no. L3065; Signalway Antibody LLC) and incubated in humidity chamber at RT for 30 min. Slides were washed with PBS, then immersed in 100 μl of FITC-conjugated goat anti-rabbit antibody (cat. no. L30113; Signalway Antibody LLC) (1:40 in dilution buffer) and incubated in the humidity chamber at RT for 30 min. After the washing procedure, 10 μl antifade mounting solution was added on each slide. Slides were covered with a rectangle coverslip (20x60 cm) and stored at 4˚C. The slides were observed with a fluorescence microscope using a B2 or B-2A filter cassette (Nikon Corporation). The FISH probes used in the present study included IGH/MAF (14q32/16q23), IGH/FGFR3 (4q16/14q32), IGH/CCND1 (11q13/14q32), glucagon-like peptide (GLP) 1q21/RB1 (1q21/13q14), GLP D13S319/TP53 (13q14.3/17p13.1), IGH (14q32), TCRAD and TCRB probes. All of the FISH probes were purchased from Wuhan Healthcare Biotechnology, Co., Ltd. A total of 200 cells were evaluated under the fluorescence microscope. The cut-off points for a positive test were 15% for probes of TCRAD or TCRB, and 8% for other probes.

Flow cytometry. The flow cytometry analysis was performed in the laboratory of the Department of Hematology, Xiangya Hospital, using bone marrow aspirate specimens. A total of 3 ml EDTA-anti-coagulated bone marrow samples were collected and kept on ice (4˚C). Samples (1.5 ml) were added into a conical centrifuge tube with 10 ml erythrocyte-lysing solution (cat. no. 348202; BD Biosciences). Next, the sample was incubated in the dark at 4˚C for 5 min. After lysis procession, the cells were preserved using cell preservation medium [composed of 500 ml RPMI1640, 25 ml 5% FBS (cat. no. 164210-500; Procell Life Science & Technology Co.,

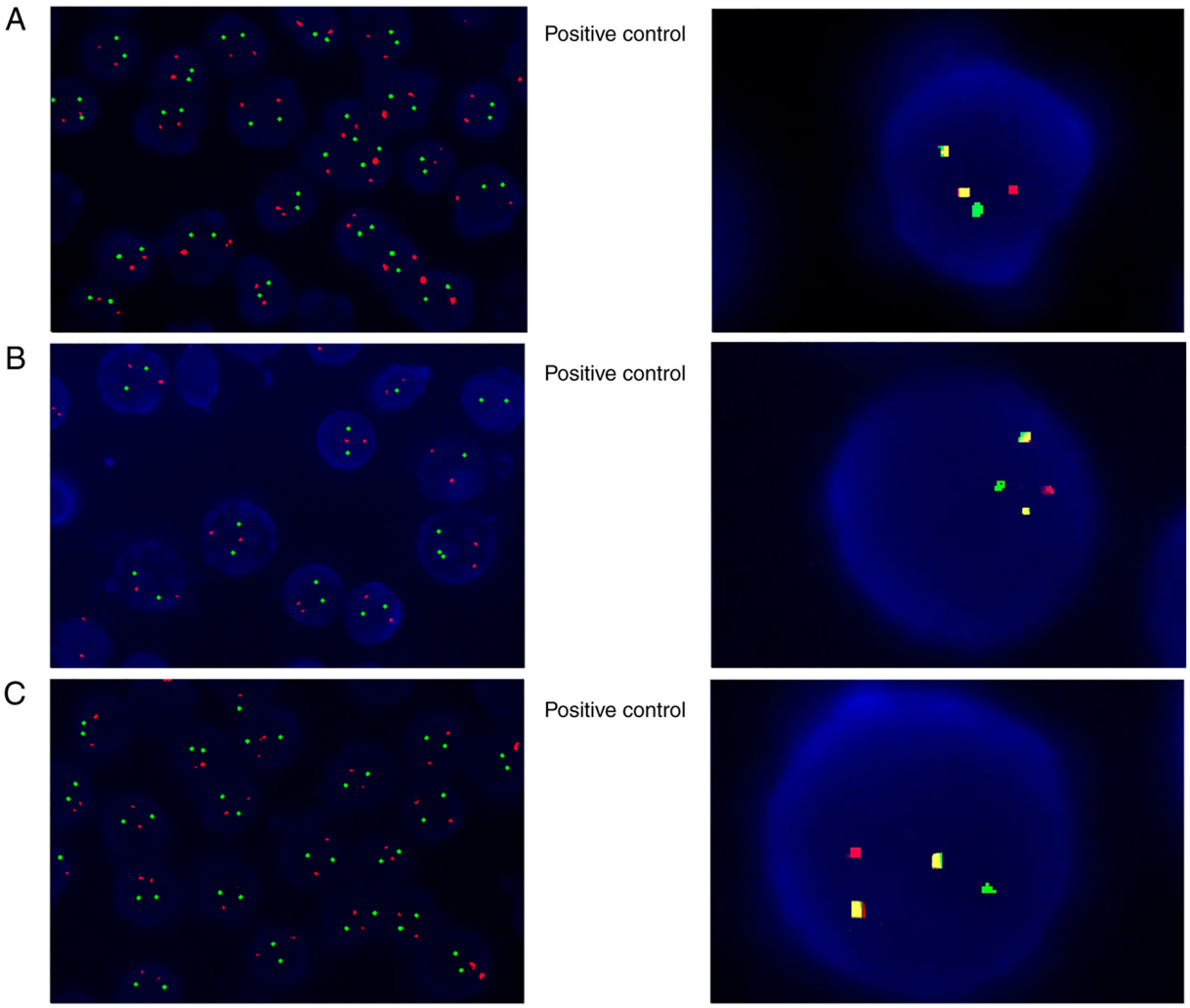

Figure 4. Images of FISH results. The FISH detection results showed that chromosomal translocations of (A) t(14;16)(q32;q23), (B) t(4;14)(q16;q32) and (C) t(11;14)(q13;q32) were negative for this patient (magnification, x100). Positive control images of corresponding translocations are on the right side of each figure (magnification, x400). FISH, fluorescence *in situ* hybridization.

Ltd.) and 5 ml Penicillin-Streptomycin solution (cat. no. DXT-0503; ScienCell Research Laboratories, Inc.)]. The cells were counted after infiltration. The cell suspension concentration was adjusted to $3.0x10^6$/ml. A total of 100 μl cell suspension was added to each tube, and then the fluorochrome-combined antibodies were added to cell suspension for incubation at 4˚C for 30 min. During cell washing, the cells were centrifuged at 400 x g for 5 min at 4˚C and resuspended in cold PBS three times. Finally, the cells were preserved with incubation in the dark at 4˚C to acquire data as soon as possible. The fluorochrome-combined monoclonal antibodies were as follows: Anti-CD7 (FITC-A), anti-CD56 (PE-A), anti-CD8 (PE-Cy7-A), anti-CD3 (APC-A), anti-CD4 (APC-Cy7-A), anti-CD45 (PerCP-A/APC-Cy7-A), anti-CD19 (PE-Cy7-A), anti-CD20 (APC-Cy7-A), anti-CD38 (APC-A), anti-CD34 (APC-A), anti-CD5 (PE-A/PerCP-A), anti-CD10 (FITC-A), sκ (FITC-A) and sλ (PE-A). All of the fluorochromes and antibodies were acquired from Becton-Dickinson and Company. Flow cytometry was performed by FACSCanto II (BD Biosciences) and data were analyzed with FACSDiva software (v7.0; BD Biosciences).

Biochemical examinations. The blood routine was analyzed by a Coulter LH 750 automatic blood cell analyzer. The biochemical tests including hepatorenal function and ferritin analysis, were performed on Beckman Coulter AU680 automatic biochemical analyzer (Beckman Coulter, Inc.). All of the examinations were conducted and analyzed by the Clinical Laboratory of Xiangya Hospital.

Immunohistochemistry (IHC) and sequencing analysis. The bone marrow specimens collected from the patient were fixed in 10% neutral formalin solution for further pathological and immunohistochemistry (IHC) analysis, as well as H&E staining, by Kindstar Global Company. The NGS of fusion genes and gene mutations, FISH probes (bcl-2, bcl-6 and myc rearrangements) and Ig gene rearrangements (PCR) were performed by Kindstar Global Company. The MYD88 L265P mutation examination was performed by Kindstar Global Company using allele-specific PCR.

Literature review

Search strategy. A comprehensive literature search was performed using the databases of PubMed (https://pubmed.ncbi.nlm.nih.gov/), Ovid Medline

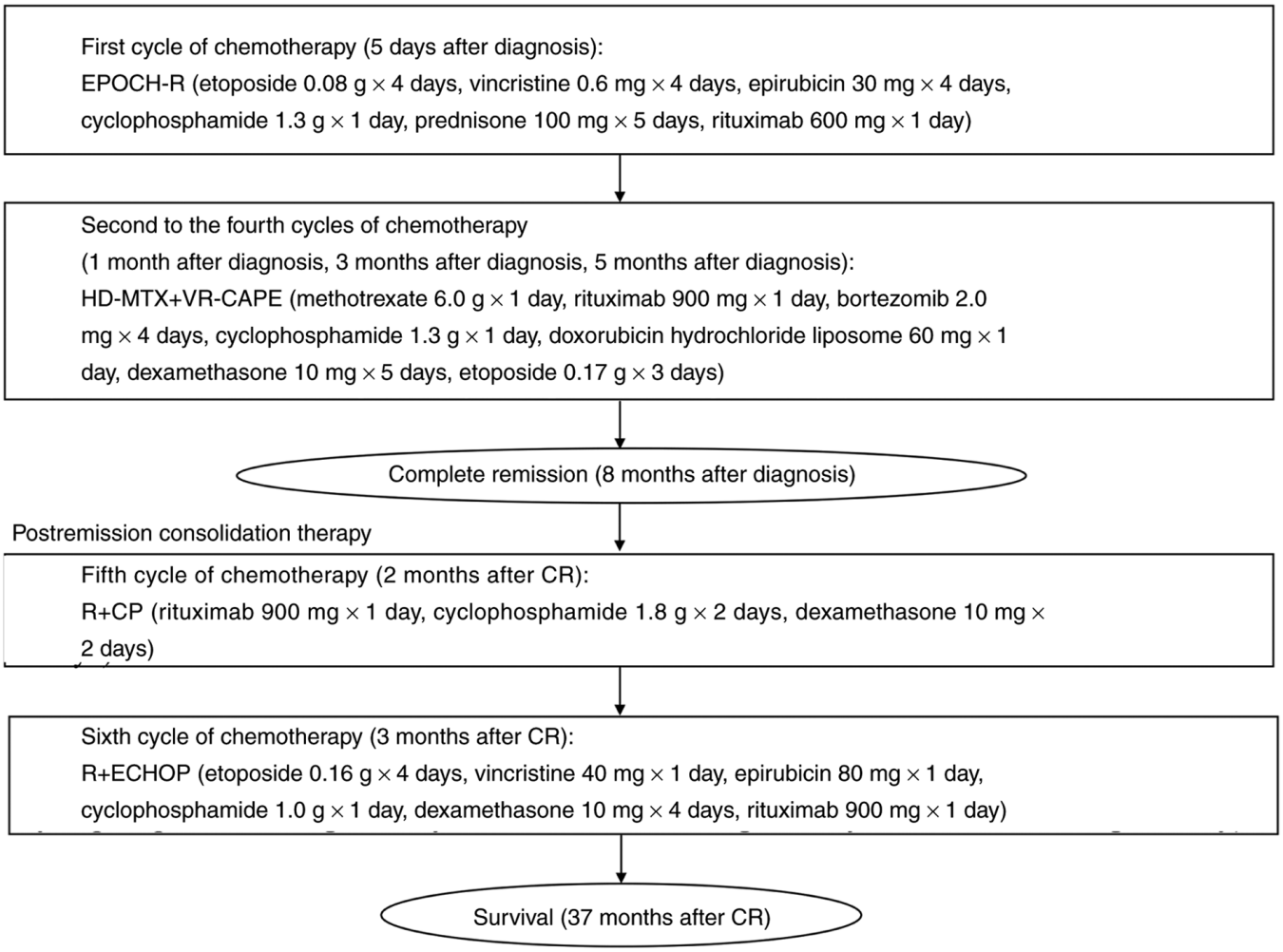

Figure 5. Chemotherapy timeline. EPOCH-R, etoposide, vincristine, epirubicin, cyclophosphamide, prednisone and rituximab; HD-MTX + VR-CAPE, methotrexate, rituximab, bortezomib, cyclophosphamide, doxorubicin hydrochloride liposome, dexamethasone and etoposide; R+CP, rituximab, cyclophosphamide and dexamethasone; R+ECHOP, etoposide, vincristine, epirubicin, cyclophosphamide, dexamethasone and rituximab.

(https://www.wolterskluwer.com/en/solutions/ovid/ovid-medline-901), Embase(https://www.elsevier.com/solutions/embase-biomedical-research), Web of Science (http://webofscience.com) and Cochrane Library (https://www.cochranelibrary.com/) between January 2002 and January 2022 with the following terms: 'Hemophagocytic syndrome(s)' OR 'hemophagocytic lymphohistiocytosis' OR 'hematophagic histiocytosis' OR 'macrophage activation syndrome(s)' OR 'cytokine release syndrome(s)' OR 'HLH' AND 'diffuse large B-cell lymphoma' OR 'non-Hodgkin lymphoma' OR 'DLBCL'.

Study identification. Studies were included if they met the following criteria: i) Refer to secondary HLH in critically ill patients; ii) concern patients with a diagnosis of histologically confirmed DLBCL; iii) provide relevant information on clinical course, treatments and outcomes; iv) are written in English; and v) contain one or multiple clinical case reports or letters. Other recognized LBCL variants, such as intravascular lymphoma, T-cell/histiocyte-rich LBCL, primary diffuse LBCL of the central nervous system (CNS) and Epstein-Barr virus-positive DLBCL were excluded due to possible different pathophysiologies. Reviewers resolved all discrepancies by discussion during the study identification process.

Discussion

Among the malignancies associated with HLH, lymphoma is the most common underlying condition. It was established that patients with lymphoma who developed HLH exhibited immune activation due to lymphoma cells or inhibitory immune function failure from the disease or treatment-induced bone marrow dysfunction (19). To the best of our knowledge, most cases of lymphoma-associated hemophagocytic syndrome (LAHS) are T-cell or NK-cell lymphomas, and HLH cases secondary to B-cell lymphoma are rarely seen in Western countries (19). Previous cohorts showed that patients with B-cell LAHS were older, but they shared parallel clinical features and laboratory data with patients with T-cell/NK-cell LAHS (20,21). Patients with B-cell lymphoma had longer survival times than those with T-cell lymphoma due to their higher response rate to treatment and the use of rituximab (22). However, HLH could be an indicator of treatment resistance in patients with malignant lymphoma, especially for patients with lymphoma originating from B cells (1). The literature review performed for the present study showed recently reported cases of DLBCL with HLH, which were similar to the clinical manifestation of the current patient,

but none of them presented with plasmacytic differentiation and MYD88 L265P mutation. Specifically, after R-CHOP chemotherapy, few patients achieved remission (23,24), and others achieved transient remission but relapsed soon after or died immediately (25,26). In the summary of a clinical case series, researchers suggested that after the combination of HLH-directed therapy and malignancy-focused interventions, treatment should be decided on a case-by-case basis (27). The detailed information of previous cases is shown in Table I.

The current case presents several intriguing findings. First, the most plausible diagnosis was DLBCL with plasmacytic differentiation. From the imaging results, lymphoma was identified. However, surgeons found that neither the adrenal gland nor the palpable lymph nodes were palpable for excision biopsy. Finally, the diagnosis of ABC DLBCL was established through a bone biopsy. A previous study revealed that different diagnoses can be made by examining lymph node biopsies and other sites of involvement, and the diagnosis concordance rate between bone marrow and lymph nodes was 84.85% (28). Most patients with discordant bone marrow involvement (BMI) progress to invasive lymphoma due to transformation of the original indolent neoplasm or benign lymphoid aggregation, and downgrading from high- to low-grade malignancy has also been observed. It is well known that BMI occurs in 10-30% of DLBCL cases. Since BMI in DLBCL is generally recognized as a high-risk advanced disease, it contributes to a higher IPI score. Unexpectedly, a previous study showed that patients with discordant BMI exhibited characteristics similar to patients without BMI (29). Patients with a concordant BMI exhibited a negative prognosis with a lower CR rate. A retrospective analysis suggested that discordant BMI might be overestimated, as some subsets of cases may be partially due to considerable morphological and immunohistological overlap, relying on individual interpretations or different bone marrow microenvironments (30). In the present study, IgM κ chain was detected in both serum and urine electrophoresis, and sκ was positive in the initial flow cytometry analysis. In addition, following the first E-POCH-R chemotherapy, flow cytometry showed that there were plasma cells expressing CD38. Although plasmacytic differentiation is unusual in DLBCL, it has been established that ABC-DLBCL is closely associated with plasmablasts that have passed through the germinal center reaction and express IgM (31). Caution is advised, and the diagnosis of DLBCL with plasmacytic differentiation must be distinguished from the transformation from lymphoplasmacytic lymphoma (LPL). However, LPL is indolent, and transformation may occur only at a frequency of 5-13% (32). Furthermore, the prognosis of DLBCL transformed from LPL appears to be worse than that of *de novo* DLBCL, with a survival time of ~2 years after transformation (33). Although the most frequent somatic mutation in LPL is MYD88 L265P, this mutation is also common in ABC DLBCL. More importantly, patients with ABC DLBCL frequently express IgM (34). However, DLBCL transformation from LPL needs to be confirmed by the pathology results of lymph node biopsies before and after transformation. As the patient in the present study did not present with any manifestation of LPL before the onset of disease, the patient was diagnosed with DLBCL with plasmacytic differentiation.

The second item of note in the present study was that it was hypothesized that the NF-κB signaling pathway was activated. In HLH, disruption of granule-mediated cytotoxicity impairs apoptosis in target cells and causes uncontrolled activation of T cells, which release proinflammatory cytokines (1). Moreover, previous data have demonstrated that high levels of serum TNF-α, IL-6 and IL-10 in B-LAHS may be due to the production of neoplastic B cells (35). There is accumulating evidence that TNF-α, a critical mediator of inflammatory immune responses, can be produced by B cells in an autocrine manner (36). The TNF-α gene is well known as an activator of NF-κB and is an NF-κB-regulated gene. The mechanism by which TNF-α mRNA translation is increased may involve strong activation of NF-κB via MYD88 in the early phase (37). It has been revealed that leukemia-initiating cells retain p65 (component of NF-κB) nuclear translocation even after serum-free culture, suggesting that constitutive NF-κB activity in cells is maintained via autonomous TNF-α secretion (38). This observation suggests that NF-κB is spontaneously activated via autocrine/paracrine TNF-α, forming an autocrine positive feedback loop between TNF-α and NF-κB activation (37,39,40). A similar situation may exist between IL-6 and NF-κB activation. Hashwah *et al* (41) reported that ABC DLBCL cells had developed complementary mechanisms that ensured constitutively active IL-6 signaling. Collectively, this evidence supports the hypothesis that NF-κB is constitutively activated by neoplastic B cells and generates an intense hyperimmune response. Above all, it is considered that tumor B cells secreted the inflammatory cytokines and activated the NF-κB consistently in the present patient.

Third, ER signaling pathway activation was mediated by lymphoma cells with plasmacytic differentiation. ER stress is obligatory in the modification and trafficking of proteins (42). In the presence of the triggers, misfolded proteins exceed the rate of protein refolding or degradation, accumulate and induce ER stress (43). During DLBCL-associated HLH, IL-6 could induce the differentiation of activated B cells into antibody-producing plasma cells (44). B-cell-specific Bcl-2 overexpression can also increase the antibody-producing cell population (45). In addition, MYD88 L265P mutations were discovered to be strongly associated with IgM secretion in LPL/IgM monoclonal gammopathy of undetermined significance (34,46). In plasma B cells, excessive production of monoclonal immunoglobulin induced ER stress. In response to ER stress, cells activate compensatory mechanisms, such as the unfolded protein response (UPR), eventually leading to ER stress-related apoptosis. If ER stress cannot be resolved, prolonged ER stress may induce the activation of the inflammatory signaling pathways, including that of NF-κB (47). Overall, constitutive NF-κB activity in tumor cells could increase tumor cell survival and resistance to cytotoxic agents (48). These data suggested that the large amount of immunoglobulin production by neoplastic B cells was also a possible explanation for the constitutive activation of ER stress and the NF-κB pathway. In the present case, there is a great possibility that the overproduction of immunoglobulin secreted by lymphoma cells with plasmacytic differentiation activated ER stress and the NF-κB pathway.

The effects of MYD88 on the NF-κB and ER signaling pathways are presented in Fig. 6. After stimulation of Toll-like receptors (TLRs) by pathogen-associated molecular patterns, MYD88 is recruited to the activated receptor via TIRAP and

Table I. Clinical features of patients with DLBCL and HLH.

First author, year	Country	Age, years	Sex	Symptoms and signs	Laboratory examination	Subtype of DLBCL	Clinical stage	International Prognostic Index	Treatment	Treatment response	Outcome from remission until publication follow-up	(Refs.)
Malkan *et al*, 2021	Turkey	32	Male	Vomiting, nausea and diarrhea, anuria, fever and hepatosplenomegaly	Pancytopenia, hypertriglyceridemia, elevated transaminases and CRP, high level of LDH and ferritin, hypercalcemia, hemophagocytosis	NA	NA	NA	HLH-2004, R-EPOCH	CR	Survival	(23)
Desai *et al*, 2020	USA	73	Female	Fever, splenomegaly	Cytopenia, hypertriglyceridemia, hyperferritinemia, hemophagocytosis	NA	IV	NA	HLH-1994, R-CHOP	ND	Death	(27)
Tang *et al*, 2020	China	64	Female	Upper abdominal pain and continuous high-grade fever	Anemia, elevated CRP and procalcitonin, liver dysfunction, lymphadenopathy	GC	NA	NA	R-CHOP	ND	Death	(59)
Wu *et al*, 2020	China	66	Male	Continuous high-grade fever with no obvious cause	Bicytopenia, increased level of ferritin, sIL-2R and triglycerides, hemophagocytosis, lymphadenopathy, splenomegaly	nGC	III B	High risk	R+ECHOP, intrathecal chemotherapy (methotrexate, cytarabine, dexamethasone)	CR	Survival	(60)
Kim *et al*, 2017	Korea	57	Male	Fever, weight loss	Bicytopenia, increased levels of ferritin, soluble CD25, LDH and β2-microglobulin, splenomegaly, hyperdiploidy and complex abnormalities, clonal rearrangement of the IGH gene	NA	NA	NA	R-CHOP	CR	Survival	(24)

Table I. Continued.

First author, year	Country	Age, years	Sex	Symptoms and signs	Laboratory examination	Subtype of DLBCL	Clinical stage	International Prognostic Index	Treatment	Treatment response	Outcome from remission until publication follow-up	(Refs.)
Patel *et al*, 2017	USA	57	Male	Weakness, fatigue, confusion, dizziness and mild jaundice	Bicytopenia, elevated creatinine, LDH, ferritin, triglycerides, liver dysfunction, coagulopathy, splenomegaly, lymphadenopathy	NA	NA	NA	Dexamethasone, ifosfamide, carboplatin and etoposide	ND	Death	(61)
Patel *et al*, 2017	USA	70	Female	Left facial weakness, fatigue, night sweats, fever, decreased appetite and weight loss	Pancytopenia, elevated LDH, ferritin, coagulopathy, hypertriglyceridemia, sCD-25	NA	IV B	NA	R-CHOP	ND	Survival	(62)
Entezari *et al*, 2015	USA	66	Male	Fevers and altered mental status without focal neurological deficits	Bicytopenia, , splenomegaly elevated LDH, serum ferritin, fibrinogen, triglyceride and sCD25, low NK cell levels, hemophagocytosis	nGC	NA	NA	High-dose dexamethasone, cyclosporine, R-CHOP	ND	Survival	(63)
Li *et al*, 2014	China	48	Male	High-grade fever, cough, weight loss, hepatosplenomegaly, lymphadenopathy	Pancytopenia, liver dysfunction, elevation of triglyceride, LDH and serum ferritin, hemophagocytosis LDH, serum ferritin	GC	IV B	High risk	High-dose methylprednisolone, cyclophosphamide, vincristine, doxorubicin and etoposide, R+ECHOP	At first CR, relapsed after 8 cycles of chemotherapy	Survival	(25)
Kuo *et al*, 2014	China (Taiwan)	51	Female	Intermit-tent fever	Anemia, elevated CRP, hemophagocytosis	NA	NA	NA	E-POCH	ND	Survival	(64)

Table I. Continued.

First author, year	Country	Age, years	Sex	Symptoms and signs	Laboratory examination	Subtype of DLBCL	Clinical stage	International Prognostic Index	Treatment	Treatment response	Outcome from remission until publication follow-up	(Refs.)
Wang *et al*, 2014	China	46	Male	Persistent fever, vibration white fingers, discontinuous arthralgia, jaundice, abdominal distention, anorexia, hepatosplenomegaly, scrotal edema and loss of body weight	Pancytopenia, coagulopathy, splenohepatomegaly, hemophagocytosis	NA	I B	NA	HLH-2004, R-CHOP	ND	Survival	(65)
Davidson-Moncada *et al*, 2013	Greek	74	Male	Increasing abdominal pain, nausea, vomiting, splenomegaly, lymphadenopathy	Anemia, liver dysfunction, coagulopathy, lymphadenopathy, elevated fibrinogen levels, serum ferritin and LDH, hemophagocytosis	NA	NA	NA	High-dose corticosteroids with rituximab, cyclophosphamide	ND	Death	(26)
Sano *et al*, 2007	Japan	63	Male	Fever and upper abdominal discomfort, hepatosplenomegaly	Pancytopenia, liver dysfunction, elevation of LDH, serum ferritin, sIL-2R, CRP, lymphadenopathy;	NA	IV	High risk	High-dose methylprednisolone, R-CHOP	CR	Survival	(66)

NA, information not available; CRP, C reactive protein; LDH, lactate dehydrogenase; Ig, immunoglobulin; sCD25, soluble CD25; sIL-2R, soluble interleukin-2 receptor; GC, germinal center; nGC, non-germinal center; CR, complete remission; ND, not determined; DLBCL, diffuse large B-cell lymphoma; HLH, hemophagocytic lymphohistiocytosis; R-CHOP, rituximab plus cyclophosphamide, doxorubicin, vincristine and prednisone; R-EPOCH, etoposide, vincristine, epirubicin, cyclophosphamide, prednisone and rituximab; R+ECHOP, etoposide, vincristine, epirubicin, cyclophosphamide, dexamethasone and rituximab.

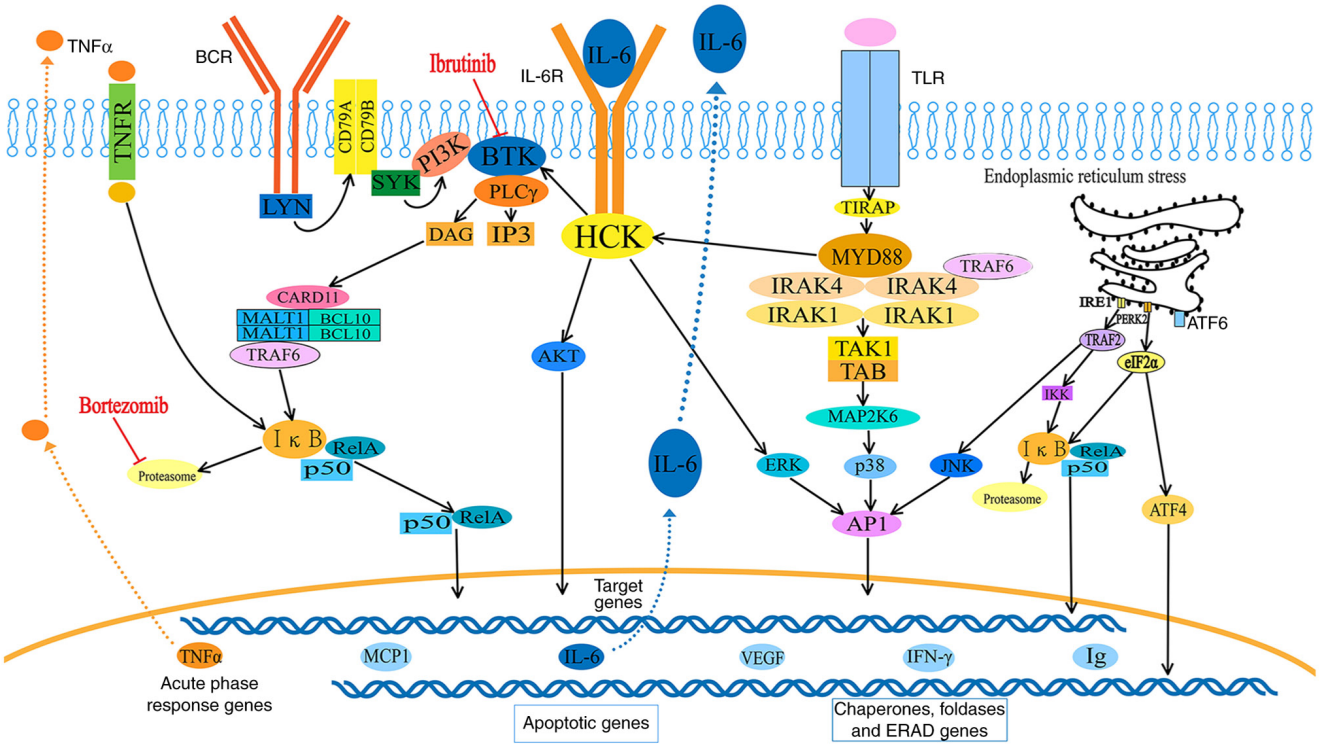

Figure 6. Proposed model indicating the effects of MYD88 innate immune signal transduction adaptor on the NF-κB and endoplasmatic reticulum stress signaling pathways. ERAD, endoplasmic reticulum-associated protein degradation.

forms complexes with interleukin-1 receptor-associated kinase (IRAK)1 and 4. IRAK1 is then phosphorylated by IRAK4, separates from MYD88, and interacts with the E3 ubiquitin ligase TNF receptor-associated factor 6 (TRAF6). On the one hand, active TRAF6 recruits and activates TAK1, which mediates phosphorylation of the IκB kinase (IKK) complex. The activated IKK complex then marks IκB for ubiquitination and proteasomal degradation, consequently releasing NF-κB dimers (49). On the other hand, active TRAF6 phosphorylates mitogen-activated protein kinase 6 (MAP2K6), and MAP2K6 activates MAPKs, including c-Jun N-terminal kinase (JNK), p38 and extracellular signal-regulated kinase (ERK), to stimulate activating protein-1 (AP-1) activity. The free NF-κB dimers and active AP-1 translocate into the nucleus to activate the expression of target genes, including IgM, TNF-α, IFN-γ, IL-6, IL-10, monocyte chemoattractive protein-1 and VEGF. Mutated MYD88 also transcriptionally upregulates and transactivates the SRC family member hematopoietic cell kinase through IL-6, which triggers the activation of Bruton's tyrosine kinase (BTK).

In response to many paraproteins, ER stress induces the UPR, which includes three pathways, the PERK-eIF2α-ATF4, IRE1-XBP1 and the ATF6 axes, which contributes to avoiding fatal ER stress through the activation of the ER chaperon and ER-associated degradation (47). Activation of the PERK/eIF-2α axis, on the one hand, results in NF-κB activation by reducing IκB protein. On the other hand, the above course increases ATF-4, which can negatively regulate the activity of NF-κB and JNK, thus increasing AP-1 (50). The IRE-1α activates TRAF-2 activates IKK or JNK, both of which activate the transcription of inflammatory genes.

It is generally agreed that ABC DLBCL presents with significantly inferior progression-free survival (PFS) and overall survival (OS) times compared with germinal center B-cell (GCB) DLBCL (51). Up to 29% of ABC DLBCL cases were originally discovered to have the MYD88 L265P mutation (52). The lymphomagenesis mechanism of L265P might facilitate its ability to drive and increase the activation of NF-κB (49). In addition to TLR-related NF-κB activity, B-cell antigen receptor (BCR)-dependent NF-κB activation is of critical importance. This constitutive NF-κB activation, which has been shown to increase lymphoma cell survival and repress chemotherapy-induced cytotoxicity, might partly explain the enhanced resistance of ABC DLBCL toward frontline chemotherapy (45). Consequently, the inhibition of NF-κB activation represents an attractive therapeutic strategy in ABC DLBCL.

Lymphoma cells in ABC tumors take advantage of BCR expression, which associates with increased tyrosine phosphorylation levels of CD79 complexes and induces sustained BCR signaling that is activated through the NF-κB pathway to sustain neoplastic proliferation (53). Hence, ibrutinib, an inhibitor of BTK, is suggested to be a treatment of ABC DLBCL (7). A recent double-blind phase III study evaluated the ibrutinib plus R-CHOP regimen in untreated ABC DLBCL, and the results showed improvements in event-free survival, PFS, and OS times, with manageable safety only in patients aged <60 years (9). In patients aged ≥60 years, ibrutinib plus R-CHOP was associated with worse outcomes and increased toxicity. A previous phase I/II trial involving patients with RR DLBCL reported that ABC tumors with BCR mutations and concomitant MYD88 mutations frequently responded to ibrutinib (4/5; 80%) (7). Notably, DLBCL with mutated MYD88 but without BCR mutations (CD79B) was unresponsive. This outcome might be associated with abnormal MYD88-activated chronic BCR signaling through

a BCR-independent mechanism or some non-genetic mechanism. However, patients who exhibited mutations in CD79B and MYD88 were associated with an increased risk of relapse and progression (54).

Lenalidomide can impact NF-κB signaling and type I interferon to improve the efficacy of ABC DLBCL. In the first phase III trial (REMARC study) comparison of lenalidomide with placebo in patients with DLBCL treated with R-CHOP, the 2-year PFS rate improved from 75 to 80% in the lenalidomide group. It is noteworthy that the patients were 60 to 80 years old, and further clinical trials need to define the effect of this agent on other age groups (8). Thereafter, a subpopulation analysis was performed to assess the impact of lenalidomide maintenance therapy (55). The results showed a trend toward improved PFS in patients undergoing dose reductions, which might be associated with bone marrow reserves.

BTZ, a proteasome inhibitor, could prevent the degradation of proapoptotic proteins in HLH and increase the protein load within the cell, consistently stimulating ER stress, and finally inducing apoptosis in cells. Furthermore, BTZ inhibited the activation of the 26S proteasome complex, blocking the degradation of IκBα. Consequently, NF-κB was unable to mediate transcription, and signaling activity was suppressed. BTZ is now widely used in the treatment of MM as an initial therapy (56). In 2009, Dunleavy *et al* (57) reported that BTZ was an effective regimen to treat DLBCL. When combined with chemotherapy, BTZ resulted in a notably higher response and median OS time in ABC than in GCB DLBCL. Notably, in an open-label, randomized controlled, phase III trial evaluating DLBCL with BTZ, there was no difference in PFS time between the R-CHOP and BTZ+R-CHOP (B+R-CHOP) groups in ABC or GCB DLBCL populations (58). Among patients with mutations that are known to be associated with the NF-κB pathway (MYD88, CD79A and CD79B), the addition of BTZ had no significant effect on their survival, although the regimen was well tolerated. However, these results might be influenced by the restricted populations and insufficient doses of BTZ. To gain insight into patient outcomes due to the extended regimen, a multicenter, open label phase I/II study for newly diagnosed $CD20^+$ DLBCL and a higher risk profile (IPI ≥2) aimed at the use of R-CHOP and a biological agent, as well as a signaling inhibitor (ibrutinib), is underway (10). This trial may reveal the responsiveness to innovative multimodality immune-signaling-biological-chemotherapy regimens in patients stratified by molecular classifiers.

In summary, the current study presented the case of a patient with HLH triggered by ABC DLBCL exhibiting plasmacytic differentiation and the MYD88 L265P mutation. Prompt recognition of HLH and an accurate diagnosis of underlying disease are obligatory and vital. Treatments not only control cytokine release but also target the underlying disorder and significantly affect the prognosis of patients. Therefore, a reliable diagnosis of lymphoma and precision therapy pointing to gene aberrations need to be examined in further research. As suggested by the present case, the application of B+R-CHOP may be successful in the treatment of the subtype of ABC DLBCL characterized by NF-κB and ER stress pathway activity.

Acknowledgements

Not applicable.

Funding

No funding was received.

Availability of data and material

The datasets used and/or analyzed during the current study are available from the corresponding author on reasonable request.

Authors' contributions

YC contributed to the analysis and interpretation of the data, as well as the drafting of the manuscript. LZ and HZ contributed to data analysis and manuscript preparation. GF contributed to the conception of the manuscript. XZ helped perform the analysis, with constructive discussions. All authors read and approved the final version of the manuscript. LZ and GF confirm the authenticity of all the raw data.

Ethics approval and consent to participate

The patient provided written informed consent for the present study.

Patient consent for publication

The patient provided written informed consent for the publication of all the data and associated images.

Competing interests

The authors declare that they have no competing interests.

References

1. Al-Samkari H and Berliner N: Hemophagocytic lymphohistiocytosis. Annu Rev Pathol 13: 27-49, 2018.
2. Yildiz H, Van Den Neste E, Defour JP, Danse E and Yombi JC: Adult haemophagocytic lymphohistiocytosis: A review. QJM: Jan 14, 2020 (Epub ahead of print).
3. Jordan MB, Allen CE, Greenberg J, Henry M, Hermiston ML, Kumar A, Hines M, Eckstein O, Ladisch S, Nichols KE, *et al*: Challenges in the diagnosis of hemophagocytic lymphohistiocytosis: Recommendations from the North American consortium for histiocytosis (NACHO). Pediatr Blood Cancer 66: e27929, 2019.
4. Henter JI, Horne A, Aricó M, Egeler RM, Filipovich AH, Imashuku S, Ladisch S, McClain K, Webb D, Winiarski J and Janka G: HLH-2004: Diagnostic and therapeutic guidelines for hemophagocytic lymphohistiocytosis. Pediatr Blood Cancer 48: 124-131, 2007.
5. Wang J, Huang J and Zeng Q: Network meta-analysis of targeted therapies for diffuse large B cell lymphoma. BMC Cancer 20: 1218, 2020.
6. Sarkozy C and Sehn LH: Management of relapsed/refractory DLBCL. Best Pract Res Clin Haematol 31: 209-216, 2018.
7. Wilson WH, Young RM, Schmitz R, Yang Y, Pittaluga S, Wright G, Lih CJ, Williams PM, Shaffer AL, Gerecitano J, *et al*: Targeting B cell receptor signaling with ibrutinib in diffuse large B cell lymphoma. Nat Med 21: 922-926, 2015.
8. Thieblemont C, Tilly H, Gomes da Silva M, Casasnovas RO, Fruchart C, Morschhauser F, Haioun C, Lazarovici J, Grosicka A, Perrot A, *et al*: Lenalidomide maintenance compared with placebo in responding elderly patients with diffuse large b-cell lymphoma treated with first-line rituximab plus cyclophosphamide, doxorubicin, vincristine, and prednisone. J Clin Oncol 35: 2473-2481, 2017.

9. Younes A, Sehn LH, Johnson P, Zinzani PL, Hong X, Zhu J, Patti C, Belada D, Samoilova O, Suh C, *et al*: Randomized phase III trial of ibrutinib and rituximab plus cyclophosphamide, doxorubicin, vincristine, and prednisone in non-germinal center B-cell diffuse large B-cell lymphoma. J Clin Oncol 37: 1285-1295, 2019.
10. Denker S, Bittner A, Na IK, Kase J, Frick M, Anagnostopoulos I, Hummel M and Schmitt CA: A phase I/II first-line study of R-CHOP plus B-cell receptor/NF-κB-double-targeting to molecularly assess therapy response. Int J Hematol Oncol 8: IJH20, 2019.
11. Wilson WH, Wright GW, Huang DW, Hodkinson B, Balasubramanian S, Fan Y, Vermeulen J, Shreeve M and Staudt LM: Effect of ibrutinib with R-CHOP chemotherapy in genetic subtypes of DLBCL. Cancer Cell 39: 1643-1653.e3, 2021.
12. Henter JI, Aricò M, Egeler RM, Elinder G, Favara BE, Filipovich AH, Gadner H, Imashuku S, Janka-Schaub G, Komp D, *et al*: HLH-94: A treatment protocol for hemophagocytic lymphohistiocytosis. HLH study GRoup of the histiocyte society. Med Pediatr Oncol 28: 342-347, 1997.
13. Hans CP, Weisenburger DD, Greiner TC, Gascoyne RD, Delabie J, Ott G, Müller-Hermelink HK, Campo E, Braziel RM, Jaffe ES, *et al*: Confirmation of the molecular classification of diffuse large B-cell lymphoma by immunohistochemistry using a tissue microarray. Blood 103: 275-282, 2004.
14. Fonseca R, Bergsagel PL, Drach J, Shaughnessy J, Gutierrez N, Stewart AK, Morgan G, Van Ness B, Chesi M, Minvielle S, *et al*: International myeloma working group molecular classification of multiple myeloma: Spotlight review. Leukemia 23: 2210-2221, 2009.
15. Yohe S and Thyagarajan B: Review of clinical next-generation sequencing. Arch Pathol Lab Med 141: 1544-1557, 2017.
16. Bartlett NL, Wilson WH, Jung SH, His ED, Maurer MJ, Pederson LD, Polley MC, Pitcher BN, Cheson BD, Kahl BS, *et al*: Dose-adjusted EPOCH-R compared with R-CHOP as frontline therapy for diffuse large B-cell lymphoma: Clinical outcomes of the phase III intergroup trial alliance/CALGB 50303. J Clin Oncol 37: 1790-1799, 2019.
17. Daudignon A, Quilichini B, Ameye G, Poirel H, Bastard C and Terré C: Cytogenetics in the management of multiple myeloma: An update by the groupe francophone de cytogénétique hématologique (GFCH). Ann Biol Clin (Paris) 74: 588-595, 2016.
18. Tian E: Fluorescence in situ hybridization (FISH) in multiple myeloma. Methods Mol Biol 1792: 55-69, 2018.
19. Campo M and Berliner N: Hemophagocytic lymphohistiocytosis in adults. Hematol Oncol Clin North Am 29: 915-925, 2015.
20. La Rosee P, Horne A, Hines M, von Bahr Greenwood T, Machowicz R, Berliner N, Birndt S, Gil-Herrera J, Girschikofsky M, Jordan MB, *et al*: Recommendations for the management of hemophagocytic lymphohistiocytosis in adults. Blood 133: 2465-2477, 2019.
21. Chang Y, Cui M, Fu X, Han L, Zhang L, Li L, Li X, Sun Z, Wu J, Zhang X, *et al*: Lymphoma associated hemophagocytic syndrome: A single-center retrospective study. Oncol Lett 16: 1275-1284, 2018.
22. Yu JT, Wang CY, Yang Y, Wang RC, Chang KH, Hwang WL and Teng CL: Lymphoma-associated hemophagocytic lymphohistiocytosis: Experience in adults from a single institution. Ann Hematol 92: 1529-1536, 2013.
23. Malkan UY, Albayrak M, Yildiz A, Maral S, Afacan Ozturk HB and Comert P: A rare case of diffuse large B-cell lymphoma-associated hemophagocytic lymphohistiocytosis. J Oncol Pharm Pract 27: 250-252, 2021.
24. Kim MS, Cho YU, Jang S, Seo EJ, Lee JH and Park CJ: A case of primary bone marrow diffuse large B-cell lymphoma presenting with fibrillar projections and hemophagocytic lymphohistiocytosis. Ann Lab Med 37: 544-546, 2017.
25. Li X, He Y, Wang D, Hu Y, Wang W and Huang R: A case of diffuse large B-cell lymphoma complicated by hemophagocytic syndrome. Clin Lab 60: 681-683, 2014.
26. Davidson-Moncada JK, McDuffee E and Roschewski M: CD5+ diffuse large B-cell lymphoma with hemophagocytosis. J Clin Oncol 31: e76-e79, 2013.
27. Desai A, Saul EE, Chapman JR, Lekakis L and Pimentel A: Adult lymphoma-associated hemophagocytic lymphohistiocytosis: A clinical case series in a predominantly hispanic cohort. J Med Cases 11: 256-261, 2020.
28. Kwoun WJ, Ahn JY, Park PW, Seo YH, Kim KH, Seo JY, Lee HT and Yoo KH: How useful is bone marrow study as an initial investigative tool without lymph node biopsy in malignant lymphoma?: Eleven years of experience at a single institution. J Clin Lab Anal 33: e22841, 2019.
29. Chigrinova E, Mian M, Scandurra M, Greiner TC, Chan WC, Vose JM, Inghirami G, Chiappella A, Baldini L, Ponzoni M, *et al*: Diffuse large B-cell lymphoma with concordant bone marrow involvement has peculiar genomic profile and poor clinical outcome. Hematol Oncol 29: 38-41, 2011.
30. Pezzella F, Munson PJ, Miller KD, Goldstone AH and Gatter KC: The diagnosis of low-grade peripheral B-cell neoplasms in bone marrow trephines. Br J Haematol 108: 369-376, 2000.
31. de Leval L and Harris NL: Variability in immunophenotype in diffuse large B-cell lymphoma and its clinical relevance. Histopathology 43: 509-528, 2003.
32. Lin P, Molina TJ, Cook JR and Swerdlow SH: Lymphoplasmacytic lymphoma and other non-marginal zone lymphomas with plasmacytic differentiation. Am J Clin Pathol 136: 195-210, 2011.
33. Boiza-Sánchez M, Manso R, Balagué O, Chamizo C, Askari E, Salgado RN, Blas-López C, Aguirregoicoa-García E, Menárguez J, Santonja C, *et al*: Lymphoplasmacytic lymphoma associated with diffuse large B-cell lymphoma: Progression or divergent evolution? PLoS One 15: e0241634, 2020.
34. Wang W and Lin P: Lymphoplasmacytic lymphoma and Waldenström macroglobulinaemia: Clinicopathological features and differential diagnosis. Pathology 52: 6-14, 2020.
35. Ohno T, Ueda Y, Nagai K, Takahashi T, Konaka Y, Takamatsu T, Suzuki T, Sasada M and Uchiyama T; Kyoto University Hematology/Oncology Study Group: The serum cytokine profiles of lymphoma-associated hemophagocytic syndrome: A comparative analysis of B-cell and T-cell/natural killer cell lymphomas. Int J Hematol 77: 286-294, 2003.
36. Aggarwal BB: Signalling pathways of the TNF superfamily: A double-edged sword. Nat Rev Immunol 3: 745-756, 2003.
37. Pękalski J, Zuk PJ, Kochańczyk M, Junkin M, Kellogg R, Tay S and Lipniacki T: Spontaneous NF-κB activation by autocrine TNFα signaling: A computational analysis. PLoS One 8: e78887, 2013.
38. Kagoya Y, Yoshimi A, Kataoka K, Nakagawa M, Kumano K, Arai S, Kobayashi H, Saito T, Iwakura Y and Kurokawa M: Positive feedback between NF-κB and TNF-α promotes leukemia-initiating cell capacity. J Clin Invest 124: 528-542, 2014.
39. Hayakawa K, Meng Y, Hiramatsu N, Kasai A, Yao J and Kitamura M: Spontaneous activation of the NF-kappaB signaling pathway in isolated normal glomeruli. Am J Physiol Renal Physiol 291: F1169-F1176, 2006.
40. Lee TK, Denny EM, Sanghvi JC, Gaston JE, Maynard ND, Hughey JJ and Covert MW: A noisy paracrine signal determines the cellular NF-kappaB response to lipopolysaccharide. Sci Signal 2: ra65, 2009.
41. Hashwah H, Bertram K, Stirm K, Stelling A, Wu CT, Kasser S, Manz MG, Theocharides AP, Tzankov A and Müller A: The IL-6 signaling complex is a critical driver, negative prognostic factor, and therapeutic target in diffuse large B-cell lymphoma. EMBO Mol Med 11: e10576, 2019.
42. Hasnain SZ: Endoplasmic reticulum and oxidative stress in immunopathology: Understanding the crosstalk between cellular stress and inflammation. Clin Transl Immunology 7: e1035, 2018.
43. Nikesitch N, Lee JM, Ling S and Roberts TL: Endoplasmic reticulum stress in the development of multiple myeloma and drug resistance. Clin Transl Immunology 7: e1007, 2018.
44. Wang HQ, Jia L, Li YT, Farren T, Agrawal SG and Liu FT: Increased autocrine interleukin-6 production is significantly associated with worse clinical outcome in patients with chronic lymphocytic leukemia. J Cell Physiol 234: 13994-14006, 2019.
45. Knittel G, Liedgens P, Korovkina D, Pallasch CP and Reinhardt HC: Rewired NFκB signaling as a potentially actionable feature of activated B-cell-like diffuse large B-cell lymphoma. Eur J Haematol 97: 499-510, 2016.
46. Treon SP, Xu L, Yang G, Zhou Y, Liu X, Cao Y, Sheehy P, Manning RJ, Patterson CJ, Tripsas C, *et al*: MYD88 L265P somatic mutation in Waldenström's macroglobulinemia. N Engl J Med 367: 826-833, 2012.
47. Maamoun H, Abdelsalam SS, Zeidan A, Korashy HM and Agouni A: Endoplasmic reticulum stress: A critical molecular driver of endothelial dysfunction and cardiovascular disturbances associated with diabetes. Int J Mol Sci 20: 1658, 2019.

48. Obeng EA, Carlson LM, Gutman DM, Harrington WJ Jr, Lee KP and Boise LH: Proteasome inhibitors induce a terminal unfolded protein response in multiple myeloma cells. Blood 107: 4907-4916, 2006.
49. Grondona P, Bucher P, Schulze-Osthoff K, Hailfinger S and Schmitt A: NF-κB activation in lymphoid malignancies: Genetics, signaling, and targeted therapy. Biomedicines 6: 38, 2018.
50. Treon SP, Xu L, Guerrera ML, Jimenez C, Hunter ZR, Liu X, Demos M, Gustine J, Chan G, Munshi M, *et al*: Genomic landscape of Waldenström macroglobulinemia and its impact on treatment strategies. J Clin Oncol 38: 1198-1208, 2020.
51. Chapuy B, Stewart C, Dunford AJ, Kim J, Kamburov A, Redd RA, Lawrence MS, Roemer MGM, Li AJ, Ziepert M, *et al*: Molecular subtypes of diffuse large B cell lymphoma are associated with distinct pathogenic mechanisms and outcomes. Nat Med 24: 679-690, 2018.
52. Visco C, Tanasi I, Quaglia FM, Ferrarini I, Fraenza C and Krampera M: Oncogenic mutations of MYD88 and CD79B in diffuse large B-Cell lymphoma and implications for clinical practice. Cancers 12: 2913, 2020.
53. Young RM and Staudt LM: Targeting pathological B cell receptor signalling in lymphoid malignancies. Nat Rev Drug Discov 12: 229-243, 2013.
54. Vermaat JS, Somers SF, de Wreede LC, Kraan W, de Groen RA, Schrader AM, Kerver ED, Scheepstra CG, Berenschot H, Deenik W, *et al*: MYD88 mutations identify a molecular subgroup of diffuse large B-cell lymphoma with an unfavorable prognosis. Haematologica 105: 424-434, 2020.
55. Thieblemont C, Howlett S, Casasnovas RO, Mounier N, Perrot A, Morschhauser F, Fruchart C, Daguindau N, van Eygen K, Obéric L, *et al*: Lenalidomide maintenance for diffuse large B-cell lymphoma patients responding to R-CHOP: Quality of life, dosing, and safety results from the randomised controlled REMARC study. Br J Haematol 189: 84-96, 2020.
56. Keats JJ, Fonseca R, Chesi M, Schop R, Baker A, Chng WJ, Van Wier S, Tiedemann R, Shi CX, Sebag M, *et al*: Promiscuous mutations activate the noncanonical NF-kappaB pathway in multiple myeloma. Cancer Cell 12: 131-144, 2007.
57. Dunleavy K, Pittaluga S, Czuczman MS, Dave SS, Wright G, Grant N, Shovlin M, Jaffe ES, Janik JE, Staudt LM and Wilson WH: Differential efficacy of bortezomib plus chemotherapy within molecular subtypes of diffuse large B-cell lymphoma. Blood 113: 6069-6076, 2009.
58. Davies A, Cummin TE, Barrans S, Maishman T, Mamot C, Novak U, Caddy J, Stanton L, Kazmi-Stokes S, McMillan A, *et al*: Gene-expression profiling of bortezomib added to standard chemoimmunotherapy for diffuse large B-cell lymphoma (REMoDL-B): An open-label, randomised, phase 3 trial. Lancet Oncol 20: 649-662, 2019.
59. Tang S, Zhao C and Chen W: Aggressive diffuse large B-cell lymphoma with hemophagocytic lymphohistiocytosis: Report of one case. Int J Clin Exp Pathol 13: 2392-2396, 2020.
60. Wu R, Deng X, Hao S and Ma L: Successful treatment of diffuse large B-cell lymphoma with secondary hemophagocytic lymphohistiocytosis by R-CHOP-E regimen: A case report. J Int Med Res 48: 300060519882233, 2020.
61. Patel R, Patel H, Mulvoy W and Kapoor S: Diffuse large B-cell lymphoma with secondary hemophagocytic lymphohistiocytosis presenting as acute liver failure. ACG Case Rep J 4: e68, 2017.
62. Patel A, Vakiti A, Chilkulwar A and Mewawalla P: Hemophagocytic lymphohistiocytosis secondary to bone marrow only B-cell lymphoma: A very rare entity with an even rarer presentation. J Hematol 6: 49-51, 2017.
63. Entezari V, Agwa E, Ruiz SJ, Lietman SA, Silver BJ and Jegalian AG: Hemophagocytic lymphohistiocytosis secondary to localized large B-cell lymphoma in a patient with history of knee arthroplasty. Leuk Lymphoma 56: 1521-1523, 2015.
64. Kuo CY, Yeh ST, Huang CT and Lin SF: Diffuse large B-cell lymphoma presenting with type B lactic acidosis and hemophagocytic syndrome. Kaohsiung J Med 30: 428-429, 2014.
65. Wang L, Zhang XH, Zhou YL and Yin XL: Hemophagocyte lymphohistiocytosis secondary to bilateral epididymal diffuse large B-cell lymphoma. Indian J Hematol Blood Transfus 30 (Suppl 1): S93-S96, 2014.
66. Sano T, Sakai H, Takimoto K and Ohno H: Rituximab alone was effective for the treatment of a diffuse large B-cell lymphoma associated with hemophagocytic syndrome. Int J Clin Oncol 12: 59-62, 2007.